

## COSMOLOGY, GRAVITATION, ASTROPARTICLE PHYSICS, HIGH ENERGY PHYSICS

<https://doi.org/10.18524/1810-4215.2024.37.312680>

SPECTRA OF LIGHTNING IN SOME WINDOWS OF  
TRANSPARENCY OF X-RAY AND  $\gamma$ -RADIATION

Doikov D.N.<sup>1,2</sup>, Doikov M.D.<sup>3</sup>

<sup>1</sup> Department of Physics, Medical Laboratory, the North Medical Center, Poria, Israel

<sup>2</sup> Department of Mathematics, Physics and Astronomy, Odesa National Maritime University, Ukraine, [dmitro.doikov@gmail.com](mailto:dmitro.doikov@gmail.com)

<sup>3</sup> Faculty of Physics and Technology, Plovdiv University "Paisii Hilendarski", Plovdiv, Bulgaria [marik.doikov@gmail.com](mailto:marik.doikov@gmail.com)

**ABSTRACT.** The processes associated with the formation of lightning and their spectra during atmospheric and volcanic phenomena were considered as a means of studying the atmospheric plasma in the X-ray and soft  $\gamma$ -ray bands. It was found that the time intervals, power of the processes, and their energy make it possible to develop new generation equipment. The lightning spectra cover the X-ray and gamma-ray bands. Hard radiation detectors have been developed and proposed for their registration. It is shown that in a physical system of emitter (lightning), absorber (medium between lightning and detector), and the detector itself, the spectral structure on the detector depends on the distance to the source and the chemical composition of the environment around thunderstorms and volcanoes. Therefore, we have calculated and found the intervals of quanta energies in which the absorber response is small. Such spectral regions are called transparency windows and are necessary for the design of appropriate detectors. In the transparency windows, the original spectra of lightning discharges are observed. To conduct field work and reduce the influence of the atmosphere during a thunderstorm, the percentage contribution of air and water extrusion in atmospheric thunderstorms was found. For volcanic discharges, silicates and  $\text{Al}_2\text{O}_3$  particles were taken. The parameters of the previously designed high-speed electrical interface suitable for operation under high voltage conditions, which is supplied to the  $\text{CsPbBr}_3$  or  $\text{Lu}(\text{SiO})_5$  detector-crystal, were obtained and described. The main economic and operational advantages of the proposed spectroscopic equipment in the field are emphasized. The operation of the high-speed spectrograph in outer space was modeled in the absence of the need for its operation without deep cooling. The transparency windows and the structure of the radiation field in the X-ray and  $\gamma$ -ray bands were calculated and systematized.

**Keywords:** hard radiation detectors, lightning, radiation deposition, X-ray transparent windows, diffusion emission, thunderstorm aerosol.

**АНОТАЦІЯ.** Процеси, пов'язані з утворенням блискавок та їх спектрів під час атмосферних та вулканічних явищ були розглянуті як засіб вивчення атмосферної плазми у рентгенівському та м'якому  $\gamma$ -діапазонах. Отримано, що інтервали часу, потужність

процесів та їх енергетика дає можливість розробляти обладнання нового покоління. Спектри блискавок охоплюють рентгенівський та гамма-діапазон. Для їх реєстрації розроблено та запропоновано детектори жорсткого випромінювання. Отримано, що у фізичній системі Випромінювач (блискавка), Поглинач (середовище між блискавкою та детектором) та сам Детектор структура спектру на Детекторі залежить від відстані до джерела і хімічного складу середовища навколо гроз і вулканів. Тому у роботі проведено розрахунки та знайдено інтервали енергій квантів, у яких відгук Поглинача малий. Такі ділянки спектрів є вікнами прозорості і необхідні для проектування відповідних детекторів. У вікнах прозорості спостерігаються вихідні спектри грозових розрядів. Для проведення польових робіт та зменшення впливу атмосфери в процесі грози було знайдено відсотковий внесок екстинкції повітря та води в атмосферних грозах. Для вулканічних розрядів бралися силікати та частки  $\text{Al}_2\text{O}_3$ . Отримані та описані параметри раніше спроектованого високошвидкісного електричного інтерфейсу, придатного для роботи умовах високої напруги, що подається на кристал-детектор  $\text{CsPbBr}_3$  або  $\text{Lu}(\text{SiO})_5$ . Підкреслено основні економічні та експлуатаційні переваги запропонованого спектроскопічного обладнання у польових умовах. Проведено моделювання роботи високошвидкісного спектрографа в умовах відкритого космосу за відсутності необхідності його експлуатації без глибокого охолодження. Розраховані та систематизовані вікна прозорості та структура радіаційного поля в рентгені та  $\gamma$ -діапазоні.

**Ключові слова:** детектори жорсткого випромінювання, блискавка, радіаційні втрати, рентгенівські вікна прозорості, дифузійне випромінювання, грозовий аерозоль.

### 1. Introduction

During the motion of quanta from the Emitter towards the Detector the processes of photoabsorption, incoherent Compton and coherent Rayleigh scattering are noticeable. As a result of photo absorption, there is also induced (characteristic) radiation. To register the latter, it is necessary to take into account that according to the presented graphs in the long-wave wing of the X-ray spectrum photo absorption

prevails. Photo absorption and corresponding resonance radiation are directly proportional. A part of quanta with energies not falling on the resonant K-lines of carbon, nitrogen and oxygen can go beyond the Absorber. The exception is the transparency window in the energy range of 280 eV (atomic oxygen), 380 eV (atomic nitrogen) and 440 eV (atomic carbon). Strong resonant scattering is observed near the marked characteristic lines. Therefore, the soft X-ray field at wavelengths of 2 nm – 4 nm is used to study microscopic particles and biological structures. To accomplish such a task, the incoming or diffuse radiation field must be sufficiently powerful. In X-ray microscopy, the role of the Emitter is played by a source of powerful cyclotron radiation. The absence of such sources can be compensated by the registration of resonance scattering near the indicated lines. Let us also note that even primitive photographic and visual observations of lightning show the stepwise character of the current motion. Such curvilinear motion of relativistic electrons leads to flashes of synchrotron radiation in the specified wavelength interval in microsecond time intervals. In other words, our designed detector should have high sensitivity in the indicated intervals of the X-ray and gamma spectrum.

## 2. The energy resource of lightning

Lightning discharges of thunderstorm and volcanic origin are formed in the zone of high potential difference  $\Delta\varphi=100$  MV, electric field strength  $E=1000$  V/m. In thunderstorm clouds, the cloud potential is formed by friction and collision of microscopic aerosols, mainly consisting of water. Initial inoculum charges can form showers and individual cosmic rays. In volcanic lightning, the main potential and inoculum charges are formed by solid particles. Mechanism of lightning formation presented in (Gurevich & Zybin, 2001; Petrov, 2021).

The Earth's atmosphere during storms and volcanic phenomena a possible to study the state of atmospheric plasma, including various aerosols. For elements with small atomic numbers the characteristic lines are in soft X-ray. The present work takes water vapor as the main aerosol component. Between the clouds pure water together with atmospheric gas are in a strong electric field with potential difference  $\Delta\varphi \approx (10^6 - 10^8)$  V. It has been shown that the hard radiation flux generated by lightning is the result of transforming the initial braking spectrum of relativistic electrons and collisions of protons, ions of C, N, and O elements with resting atoms of the medium. Both currents consisting of ions and electrons are directed in opposite directions.

The gamma and X-ray radiation of lightning reaches the detectors with strongly attenuated long-wave part. At energies less than 1 keV, practically all energy of long-wavelength X-ray quanta is spent in photo-ionization of surrounding water vapor. However, in the wavelength range (2.34 – 4.4) nm we have bound energies (530 – 280) eV. There is a transparency window with characteristic K-lines of C, N, O atoms. We propose a method and compose a model for registration of radiation fluxes in the window of water transparency. This allows us to study the plasma in which intensive ionization processes occur by the joint action of photons and impact ionization of atoms by electrons

and protons. The protons and electrons experience collisions with target atoms – C, N, O. It was obtained that at sufficiently high saturation with water vapor around the lightning. Its long-wave part is cut off in the X-ray spectrum. The relationship between water vapor content and radiation intensity at the receiver is described. The concurrence of the processes of scattering, absorption of X-ray quanta and formation of induced secondary quanta (characteristic emission of C, N, O elements) is responsible for the formation of the observed diffuse (bulk) X-ray fluorescence (Kozirev et al., 2011), (Doikov & Doikov, 2023).

For simulation of the process of nucleation of electron and hadronic (p,  $\alpha$ -particles + C, N, O - ions) currents was carried out in the framework of the Geant4 DNA code (Inserti et. al., 2010). Concurrently, the formation of X-ray and UV fluorescence was monitored. All necessary spectroscopic constants for the media in which the processes under consideration took place above described processes took place in a strong electric field with a potential difference of  $\Delta\varphi = (10^6 - 10^8)$ V, which leads to the intensity  $E=(10^3 - 10^5)$  V/m. A comparison with the laboratory experiments in (Kozirev et al., 2011) has been made. On the basis of modeling of various types of lightning using spectra of lightning in the X-ray range are constructed and conclusions are drawn concerning the application of this method in the study of explosive processes on the surface of White Dwarfs (WD).

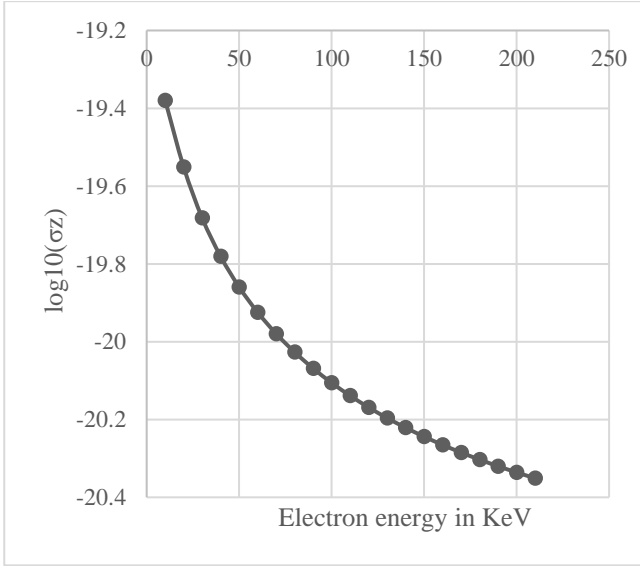
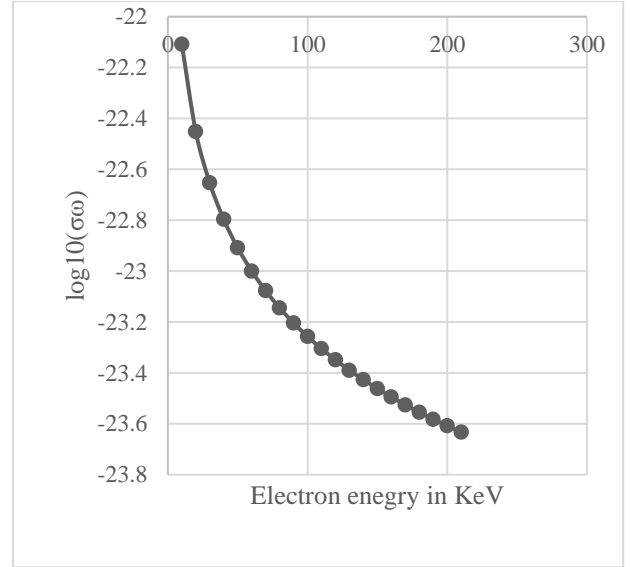
## 3. X-ray transport in thunderstorm clouds

Lightning generates X-ray and gamma radiation in a wide range of the spectrum. It is caused by braking of fast (in some cases relativistic) electrons. Appearing inside the current cylinder, the quanta cross its surface and are directed to the detector. Further quanta experience random multiple acts of Compton and Rayleigh scattering, or experience photo absorption. In this case, the radiation field is determined by the elemental composition of air (in the used codes it is macro command G4\_Air) and the fraction of water vapor (G4\_Water). If lightning is formed in volcanic clouds, it is necessary to specify the distribution of silicon and phosphorus along the propagation of quanta. In rain clouds, the inoculum of free ions is formed as a result of CR ionization losses. In volcanic ones as a result of mutual friction of the solid fraction.

### 3.1. Formation of radiation in lightning

The current discharge in lightning has a powerful transient, mile-microsecond pulse character. The electronic component of the current at the specified values of  $\Delta\varphi$  has velocities sufficient for the formation of braking radiation. This leads to the formation of a continuous spectrum of hard radiation. This spectrum is limited on the short wavelength side by soft  $\gamma$ -radiation. The target atoms for fast electrons are C-N-O elements, the maximum of the spectral distribution of the braking radiation of which is more likely to fall in the entire X-ray range.

The electron kinetic energy spectrum  $W(\lambda)$  is essentially relativistic. The external electric field has a strength  $E \cong 10^2 - 10^3$  V/m. The maximum current amplitude at the peak of discharge reaches  $3 \cdot 10^4$  A. During discharge,  $\Delta\varphi$  drops to zero. According to (Gurevich & Zybin, 2001) and


 Figure 1: Impact ionization cross section  $\sigma_Z$ 

 Figure 2: Bremsstrahlung cross section  $\sigma_\omega$ 

(Petrov, 2023) the formation of the current pulse is determined by “fleeing” electrons. A  $\delta$ -shaped peak appears in the spectrum  $W(\lambda)$  at this moment. To determine the time evolution of  $W(\lambda)$ , it is necessary to take into account all channels of energy acquisition and loss by fast electrons. As an initial approximation, we choose the Maxwell velocity distribution. Then let us apply the corresponding potential difference  $\Delta\varphi$  to the cylinder in which the lightning nucleates. Among the main channels of energy losses, we note the losses on Bremsstrahlung radiation with cross section  $\sigma_\omega$  and the cross section of ionization of K-level C-N-O atoms is  $\sigma_Z$ .

$$\sigma_\omega = \frac{16\pi e^2}{3hc^2} \left( \frac{Ze^2}{mV_0} \right)^2 \ln^2 \left( \frac{2mV_0^2}{\gamma Ze^2 \omega_{mn}} \right) \quad (1)$$

$$\sigma_Z \cong \frac{10^{-24} \text{cm}^2}{I_Z E(E+2)} \left\{ 2 + (E+1)^2 \ln \sqrt{\frac{E(E+1)}{I_Z}} - \frac{I_Z}{E} \left[ (E+2)^2 + 2(2E+1) \ln \frac{E}{E_Z} - 2 \right] \right\} \quad (2)$$

Here  $I_Z = \frac{E_Z}{mc^2}$ ,  $E = \frac{mV_0^2}{2mc^2}$ ,  $E_0 = 537 \text{ eV}$ ,  $E_N = 405 \text{ eV}$ .

At a quantum energy of 10 keV, the characteristic cross section value is  $\sigma_Z \cong 5 \cdot 10^{-20} \text{cm}^2$ , a  $\sigma_\omega/\sigma_Z \cong 10^{-3}$ . Fig. 1 and Fig. 2 show the cross sections  $\sigma_\omega$ ,  $\sigma_Z$  in logarithmic scale normalized to the electron scattering cross section  $\sigma_T$ .

Diffuse X-ray emission. The initial spectrum of hard radiation undergoes further evolution during the discharge process. For this purpose, the macro commands of Weber G codes (see Weber G link) are addressed to cross sections of characteristic processes of interaction of quanta with matter. The structure of the nonlinear behavior of cross sections of all energy loss channels leads to a shift of the maximum of the spectral distribution of their energy towards longer wavelengths. Modeling of X-ray quantum beams shows that their spectrum is gradually filled with a diffuse X-ray component.

A similar effect occurs in observations of the intrinsic diffuse radiation of planets caused by the Sun's radiation. The calculations of the spectrum of hard radiation coming from lightning suggest that its quanta at the initial moment of time cross the walls of the current cylinder. At this moment the mechanisms of coherent and incoherent scattering of hard radiation are switched on. Rayleigh scattering of sunlight on molecules is replaced by the scattering of hard radiation on atomic structures.

In this case the extinction cross section  $k$  is defined through the cross sections of Compton scattering  $\sigma_c^Y(\varepsilon)$  and atomic photo effect  $\sigma_{af}^Y(\varepsilon)$ . Similarly to formulas (1) and (2) for the energy of quanta we substitute  $\varepsilon = E_\gamma/m_e c^2$ .  $E_\gamma$  is the energy of a hard radiation photon.  $m_e c^2$  is the rest energy of the electron. Let us denote by  $\sigma_T = 6.65 \cdot 10^{-25} \text{cm}^2$  the cross section of elastic, Thomson scattering of photons on electrons. Then we have

$$k = \sigma_{af}^Y(\varepsilon) + \sigma_c^Y(\varepsilon). \quad (3)$$

In the framework of the adopted notations, we will write down:

$$\sigma_{af}^Y(\varepsilon) = \left( \frac{32}{\varepsilon} \right)^{3/2} \alpha^4 Z^5 \sigma_T, \quad (4)$$

$$\sigma_c^Y(\varepsilon) = 2\sigma_T \left[ \frac{1+\varepsilon}{\varepsilon^2} \left( \frac{2(1+\varepsilon)}{1+2\varepsilon} - \frac{1}{\varepsilon} \ln(1+2\varepsilon) \right) - \frac{1}{2\varepsilon} \ln(1+2\varepsilon) - \frac{(1+3\varepsilon)}{(1+2\varepsilon)^2} \right]. \quad (5)$$

For each individual quantum within the free path length all its characteristics and trajectory are tracked by the Monte Carlo method. Such quanta form secondary electrons, which in turn ionize the medium along their trajectory. The flux of quanta and particles formed in this way arrives at the detector crystal. The calculation results are presented in Fig. 3 and Fig. 4.

It follows from the results shown in Fig. 6 that in the conditions of thunderstorm clouds Compton scattering takes the highest values in the long-wave part of the spectrum.

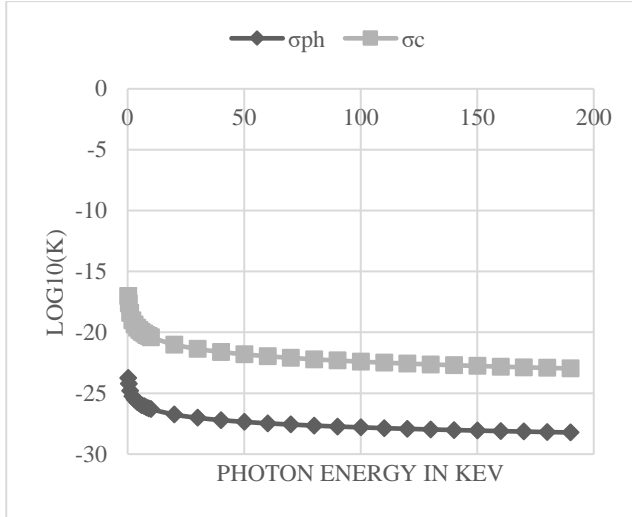


Figure 3: Diffuse photoelectric  $\sigma_{ph}$  and Compton scattering  $\sigma_c$

It follows from the results shown in Fig. 6 that in the conditions of thunderstorm clouds Compton scattering takes the highest values in the long-wave part of the spectrum. The short-wave part of the X-ray spectrum of lightning is practically undistorted up to energies of 50 keV. If we consider the cloud as a fog with relative humidity, the free path length of X-ray quanta between two acts of Coulomb scattering takes the values shown in Fig. 5. During rain, it is necessary to take into account the percentage of drops in the thunderstorm cloud.

Let us take into account that the average concentration of water in raindrops is three orders of magnitude higher, then the obtained values of  $f_{pass}$  should be on average  $10^3$  times higher and, accordingly,  $f_{pass}$  is the same number of times smaller. It follows from Fig. 3 – Fig. 5 that the main type of X-ray scattering is the incoherent Compton scattering given by the formula. Moreover, at each act of scattering it is necessary to recalculate the wavelength of the quantum after scattering –  $\lambda'$ . If before scattering we have a wavelength  $\lambda$  and a scattering angle  $\theta$ , then the relation is satisfied:

$$\lambda' = \lambda + \frac{h}{mc^2}(1 - \cos\theta) = \lambda + 2,4 \cdot 10^{-3} \text{HM} \cdot (1 - \cos\theta) \quad (6)$$

At the wavelength interval from 0.12 to 0.06 nm, the peak of Compton scattering in water is noticeable and a rapid decrease in photo absorption begins. In this interval, the appearance of X-rays scattered mostly by oxygen and nitrogen is expected. The quantum beam attenuation coefficients due to photo absorption, Compton and Rayleigh scattering are presented in Fig. 6. In the presented resources we calculated scattering angles  $\theta$  were set by the Monte Carlo method in the range from 0 to  $\pi$  radians. The results of averaging cross sections of beams containing 100 X-ray quanta each are presented in Fig. 7. The calculations were performed for the thickness of the equivalent water layer of 1 cm. The modeling results show general trends in the dependence of attenuation coefficients on the energy of quanta predicted by the formulas. However, for spectral analysis of the investigated objects the results of accurate

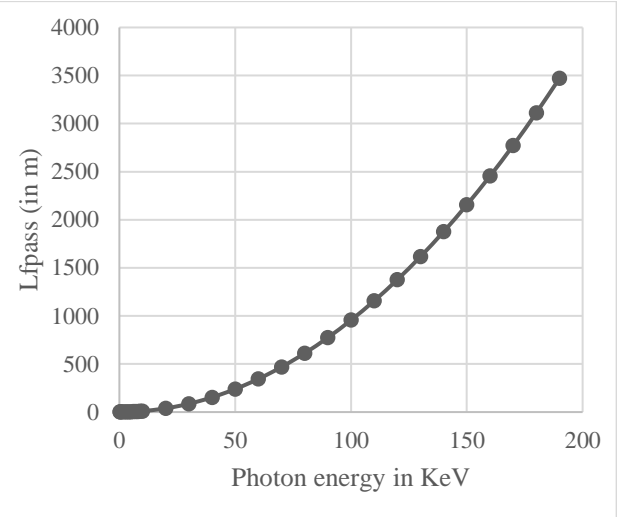


Figure 4: Free path lengths X-,  $\gamma$ -rays photon in pure air (G4\_Air)

“ab initio” The calculations in Fig. 6 are applicable. In the future, we will use them for quantitative analysis of X-ray spectra of lightning to determine the content of elements in lightning during lightning discharge (Kozirev et al., 2011).

### 3.2 Characteristic radiation

Quanta of soft X-ray radiation occupy wavelengths of 0.01 nm – 10 nm. In this interval all quanta from electron transitions to the free K-level of atoms, which are part of air and water droplets, occur.

If the energies of the quanta are adjacent to the edge of the lines arising in the photo effect, strong resonance scattering is observed, and inside the absorption lines. Along with elastic scattering, X-ray quanta also experience incoherent scattering in the form of Compton scattering.

The process of photo ionization of aerosol represented by water droplets of carbon, nitrogen and oxygen, which are part of air. Scattered quanta is mainly determined by photo ionization of K-shells of atoms. Near these lines we have resonant scattering of diffuse radiation.

Next, for air under normal conditions and for a given concentration of raindrops, we estimate the number of such collision acts on the path of the X-ray quantum to the detector. We need to trace the shift of the X-ray spectrum in the region of the “transparency window” of water.

## 4. Detector construction

The design of detectors-spectrographs of hard radiations requires fulfillment of a number of requirements to their operation. In particular, for diagnostics of the described processes in thunderstorm and volcanic lightning requires the closest possible placement of equipment to the object of study. In high mountain conditions at altitudes higher than 1 km the distance from the Detector to the Emitter can reach 1 km on average. The thunderstorm cloud aerosol at such scales completely absorbs the long-wave part of X-ray radiation. Quanta with energies up to 100 keV experience complete Compton scattering. In this range we have diffuse

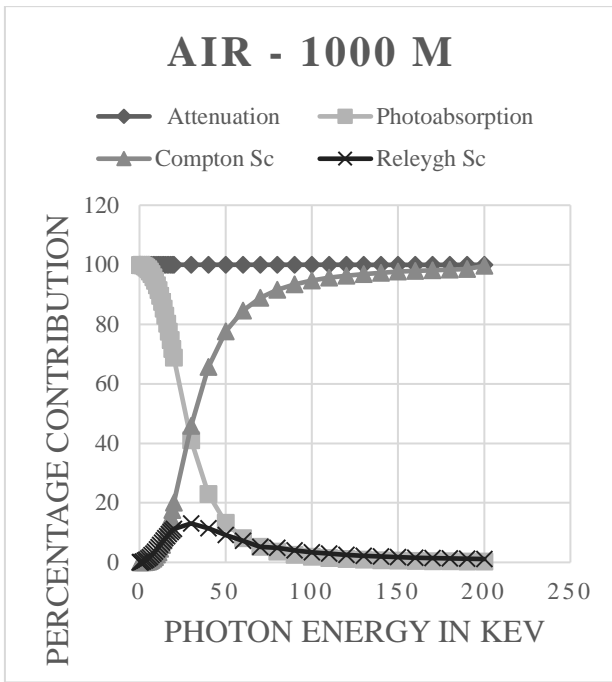


Figure 5: Radiation field after crossing 1 km of pure air

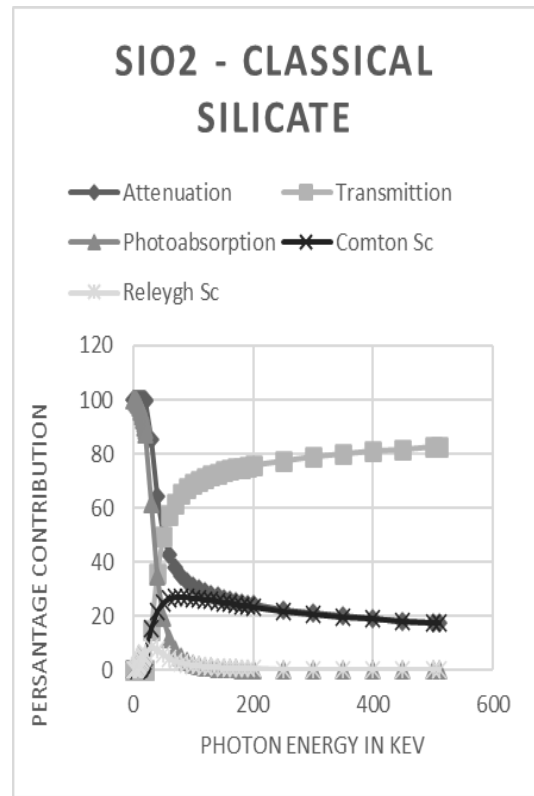


Figure 7: Ibid after crossing of 1cm classical silicate

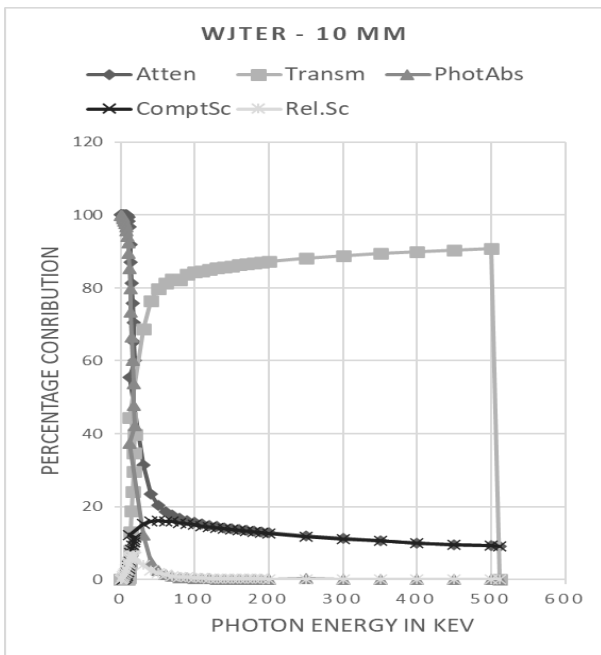


Figure 6: Radiation field spectra after crossing 1 cm of pure water

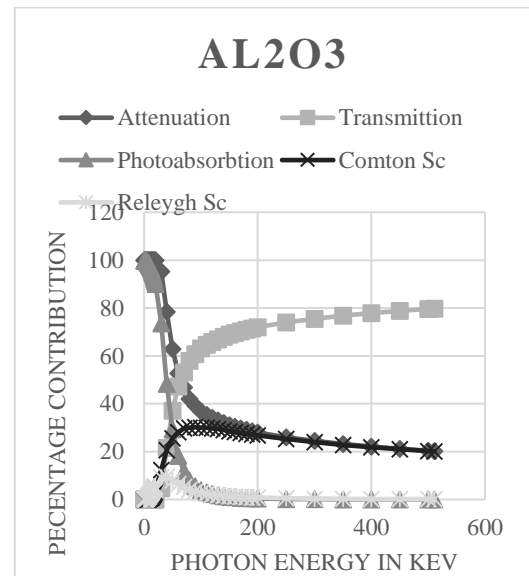


Figure 8: Ibid after crossing of 1cm Al<sub>2</sub>O<sub>3</sub>

X-ray luminescence. The directional flux of gamma ray quanta is expectedly registered by the detector. The calculated shape of the lightning detector includes a thin quartz plate and a cube with an edge of 0.5 cm – 1 cm. This geometry allows for guaranteed registration of lightning radiation in the range of 0.01 MeV – 1 MeV. Semiconductor crystals have been widely studied for this purpose CsPbBr<sub>3</sub> и Lu(SiO)<sub>5</sub>. The obtained results on design and modeling of detectors are presented in Fig. 9 and Fig. 10. The number of quanta in the flux is assumed to be 50. The flux defocus-

ing is carried out by incoherent Compton scattering. A part of quanta is reflected back (by 180°). Visualization of particle trajectories is described in (Inserti et. al., 2010). To determine the efficiency of the crystal, the fraction of the flux energy spent on the actual ionization of the crystal substance was determined. A detailed study of these issues in (Doikov, 2022) allows us to obtain the values of the current pulse amplitude (1 nA – 10 nA) and the time scale of its formation (1 μs – 100 μs).

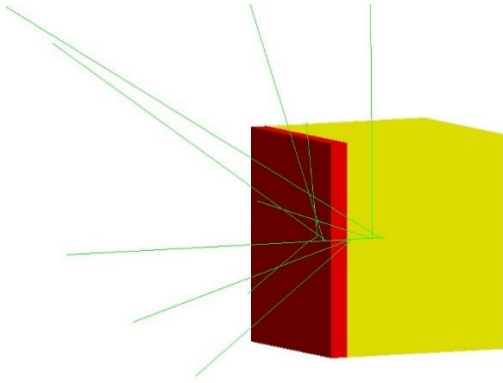


Figure 9: SiO<sub>2</sub> 0.1 mm and CsPbBr<sub>3</sub> 10 mm target length.  $E_{\gamma} = 511$  keV

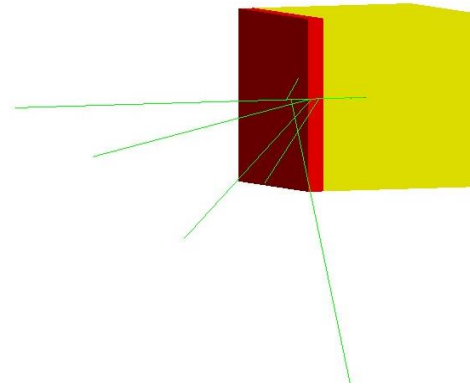


Figure 10: SiO<sub>2</sub> 0.1 mm and Lu(SiO)<sub>5</sub> 10 mm target length.  $E_{\gamma} = 100$  keV

## 5. Discussion

The transfer of hard radiation formed by lightning is accompanied by a noticeable change in its shape. The most informative results are obtained with high-speed X-ray and gamma-ray spectrographs at the flash peak. This means that the equipment we are developing should operate in the monitoring mode. This means that the electronic interface should only be triggered when a sufficiently powerful pulse is received that the signal-to-noise ratio is maximized. The convenience in carrying out mass in-situ measurements of lightning spectra and images from stationary high-altitude observatories significantly increases the chances of obtaining high-quality results.

## 6. Conclusion

In the present work we obtained original results necessary for diagnostics of hard radiations formed at fast thermonuclear processes. The energy resource of lightning in sounder storms and volcano causes a whole chain of thermonuclear processes and their accompanying bursts of hard radiation. Presented in Fig. 5 – Fig. 8 predicted the presence of an intense component in the spectrum of scattered X-rays and the presence of strong self-absorption near the spectral windows of transparency. Multiple scattering of hard radiation quanta creates specific images of lightning and requires a separate approach to their visualization.

*Acknowledgements.* D.D., would like to thank Tsafon Medical Center for material support in writing this paper. M.D. and D.D. thank the Geant4-DNA project (Inserti et al., 2010) and Dr. G. Weber for the opportunity to use the open-source code of their programs.

*Athor contribution:* DD: sections 2; MD: sections 3,4,5. In sections 1, 6 of the article the authors' contributions are the same.

## References

- Doikov D.N., Doikov M.D.: 2023, *OAP*, **36**, 51-58.  
 Doikov M.D.: 2022, *OAP*, **35**, 24-29.  
 Gurevich A.V., Zybin K.P.: 2001, *Usp. Phys. Nauk*, **171**, № 11, p. 1177.  
 Inserti S., Balanchino G., Bernal M. et al.: 2010, *Int. J. of Modeling, Simulation, and Scientific Computing*. 01, 02, 157-178. DOI: 10.1142/S179396231000012  
 Kozirev A.V., Tarasenko V.F., Baksht E.H. et al.: 2011, *Letter in JTF*, **37**, 22.  
 Petrov N.I.: 2021, *Scientific Report* **11:19824**, <https://doi.org/10.1038/s41598-021-99336-3>.  
 Weber G. [https://web-docs.gsi.de/~stoe\\_exp/web\\_programs/x\\_ray\\_absorption/index.php](https://web-docs.gsi.de/~stoe_exp/web_programs/x_ray_absorption/index.php)